

# Ultrahigh Power Graphene Based Supercapacitor

Binghe Xie, Peichao Zou, Cheng Yang\*  
Graduate School at Shenzhen  
Tsinghua University  
Xili University Town, Shenzhen, China  
E-mail: yang.cheng@sz.tsinghua.edu.cn

**Abstract**—Supercapacitor as a type of new energy storage device has important applications in the development of smart electronics and vehicles, which can provide a high current density to drive the devices. Recently, although graphene has been considered as a very promising electrode material for supercapacitors, the poor control of the dispersion of graphene and the limited way of electrode preparation process severely hinder its power performance. Here, we report a supercapacitor technology with ultrahigh power combining the electrochemically reduced graphene oxide deposited on nickel nanocone array with printed ethylene vinyl acetate cofferdams. The supercapacitor showed excellent rate performance, ultrahigh power density (1230 mWh/cm<sup>3</sup>) and high ionic mobility, especially when compared to those with separator. In light of the simple process (electrochemical-deposition and stencil printing, etc.), this technology can meet the demand of applications with high power density and inspire the development of other energy storages to achieve better performance.

**Keywords**—ultrahigh power, graphene, supercapacitor

## I. INTRODUCTION

Owing to many intriguing characteristics, such as flexibility, lightweight and small size, wearable electronic devices have been rising to lead the trend of consumer electronics. In this run, the small energy storage units with high performance have become an indispensable part. Supercapacitor, featured with high power, can provide strong electric current to support the device work, which has been intensively investigated [1]. Recently, graphene, a typical two-dimensional carbon material, which shows a large specific surface area (2675 m<sup>2</sup>/g) and ultrahigh theoretical specific capacitance (550 F/g), has been widely considered as an ideal active material for supercapacitor [2]. Previous works about graphene based supercapacitors exhibited excellent specific capacitance, cyclability, rate performance and superior energy density, while the power density failed to achieve better performance [3, 4]. Recent works about manipulating the orientation and assembly of graphene depicted a new horizon of the graphene based energy storage devices [5, 6]. For example, a constant electric field is able to trigger the self-assembly and reduction of graphene oxide, rendering the electrochemical reduction of graphene oxide (ErGO). The ErGO are assembled vertically on the substrate (acting as the current collector), which can greatly accelerate the migration of ions and improve the power density and rate performance of the supercapacitor.

Conventional supercapacitors have a sandwich structure, which are assembled with a separator to prevent the contact between two electrodes, which is disadvantageous for fast migration of ions [7]. Although planar supercapacitors can

effectively shorten the diffusion pathway of ions, the gel electrolyte hinders the high-speed motion of ions as well, which inevitably limited the power density of supercapacitor [8]. To date, developing graphene based supercapacitor (GS) with an ultrahigh power density is still a challenging task.

Here we reported a GS with ultrahigh power density by combining ErGO deposited on nickel nanocone arrays (NCAs) with a unique packing technique. Macroporous ErGO network can homogeneously form on NCAs as a binder-free electrode, which can facilitate ion transports. In term of packing process, the conventional stencil printing and ethylene vinyl acetate glue were employed to construct a cofferdam, which not only effectively prevented short circuit, but also guaranteed the high mobility of ions. A series of tests demonstrated that GSs assembled with 0.5 M Na<sub>2</sub>SO<sub>4</sub> electrolyte showed excellent capacitance characteristics, rate performance, superior ions' mobility and ultrahigh power density (1230 mW/cm<sup>3</sup>). As simple as the process is, this technology can meet the demand of applications with high power density and inspire the development of other energy storages to achieve better performance.

## II. EXPERIMENTAL

### A. Synthesis of GO and nickel nanocone array

The GO was prepared by a modified Hummers method, and the synthesis of nickel nanocone array was according to the previous work [9, 10].

### B. Preparation of ErGO electrode

A simple electrochemical-deposition setup with two-electrode configuration was used to fabricate macroporous ErGO network on NCAs substrate. Briefly, a GO solution mixed with 0.1 M LiClO<sub>4</sub> was used as the electrolyte. NCAs were used as the working electrode, while platinum foil was used as counter electrode, which was applied with a constant voltage ranging from -2.8 V to -3.2 V for 10 - 120 minutes. It should be noted that Ar<sub>2</sub> was constantly blown into GO solution to remove residual O<sub>2</sub> during the electrochemical-deposition, which was conducive to form uniform ErGO layer. NCAs deposited with ErGO samples were washed carefully with DI water for several times and freeze-dried for further characterizations.

### C. Fabrication of symmetric supercapacitor

Ti plates deposited with NCAs were used as current collector and EVA (polyethylene vinyl acetate, working temperature 80 °C) glue acted as the hot-melt binder. After constructing EVA cofferdams on NCAs via stencil printing technique, the samples were air-dried at room temperature to

solidify the EVA glue. After the ErGO was deposited onto NCAs, the samples were cleaned by DI water and air-dried. Two identical ErGO electrodes with EVA cofferdams were soaked with 0.5 M Na<sub>2</sub>SO<sub>4</sub> and laminated together immediately to form a symmetric supercapacitor by hot-pressing at 80 °C under 8 Pa of compression strength for three minutes. As a control sample, the aqueous supercapacitor with separator was fabricated with two ErGO electrodes (the area is same with the supercapacitor mentioned above) and a separator between two electrodes was integrated to prevent short circuit. Tape was used to package and avoid the leakage of electrolyte.

#### D. Materials characterizations and electrochemical measurements.

The morphologies of both NCAs and ErGO were characterized by scanning electron microscopy (SEM, Hitachi S-4800, Japan). The structure of samples was studied by X-ray diffraction (XRD, RINT2000V/PC, Bruker DS, Germany) and Raman spectroscopy (LabRAM HR800, HORIBA Jobin Yvon, Japan).

Cyclic voltammetry (CV), galvanostatic charging/discharging (GCD) and electrochemical impedance spectroscopy (EIS) of the as-prepared samples were investigated on an electrochemical station (VMP3, Bio-Logic, France). The applied potential window of CV and GCD was in the range from 0 V to 0.8 V. The EIS study was conducted in the frequency range between 100 KHz and 0.01 Hz with an amplitude of 5 mV at an open-circuit potential. The energy and power density (E and P) of supercapacitor were calculated by the equations below:

$$C_{V_{total}} = \frac{I \cdot \Delta t}{\Delta U \cdot V_{total}} \quad (1)$$

$$E = \frac{C_{V_{total}} \cdot (\Delta U)^2}{2 \cdot 3600} \quad (2)$$

$$P = \frac{E}{t} \quad (3)$$

Where I is the applied current, Δt is the discharge time, ΔU is the operating voltage window, and V<sub>total</sub> is the total volume of supercapacitor, including ErGO electrode, gel electrolyte and EVA cofferdams.

### III. RESULTS AND DISCUSSION

The nickel nanocone array was prepared by one-step electro-deposition, which was used as current collector, aiming at providing larger specific area and superior bonding force [10]. In term of ErGO deposited on NCA, a simpler electrochemical-deposition method with two-electrode configuration was applied compared to previously reported three-electrode configuration, which was conducive to obtain electrode with larger area. The formation of ErGO was confirmed by XRD and Raman characterizations, as shown in Fig. 1. An intense peak located at 2θ = 11° in the XRD pattern of GO represents the typical structure of GO sheets, while a new peak appears at 2θ = 24° after electrochemical-deposition,

reflecting the conversion of GO to ErGO [11]. In addition, the information about formation of ErGO can be provided by Raman spectra. The intensity ratio of I<sub>D</sub>/I<sub>G</sub> increased from 0.97 to 1.11 after the reduction process, which is a typical phenomenon for reduction of GO, which could be attributed to the increased amount of small conjugated domains [5].

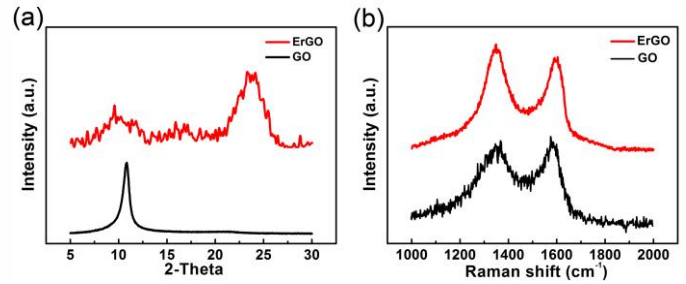


Fig.1 XRD (a) and Raman (b) of ErGO and GO

During the electrochemical-deposition process, GO sheets tend to deposit vertically on NCA owing to the perpendicular electric field applied to NCA. The over-view and side-view SEM images of ErGO on NCA are displayed in Fig. 2. ErGO exhibited a macroporous network feature and some ErGO were perpendicular to the substrate, which enabled the ions easier to access the internal ErGO network and provided fast transport channels for ions. From the cross-sectional observation, the ErGO was successfully deposited on NCA, and the thickness of ErGO layer was about 8 μm, which contributed to deliver higher areal capacitance.

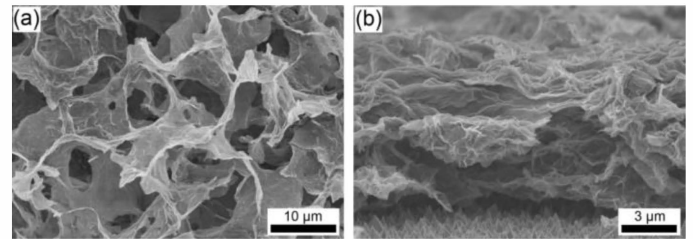


Fig.2 over-view (a) and side-view (b) of ErGO on NCA

As shown in Fig. 3a, the NCAs deposited with ErGO exhibited a darker color than NCAs collector, suggesting the successful formation of ErGO on NCAs. In order to fabricate a supercapacitor with ultrahigh power density, the EVA cofferdams were constructed on NCAs by stencil printing technique (Fig. 3b). After the solidification of EVA cofferdams, the NCAs with EVA cofferdams were immersed to GO electrolyte and applied constant voltage to form uniform ErGO layer (Fig. 3c). After rinsed with 0.5 M Na<sub>2</sub>SO<sub>4</sub> (aqueous) electrolyte, two identical ErGO electrodes were assembled to a symmetric supercapacitor with the thickness about 65 μm. (Fig. 3d) In this process, the EVA cofferdams acted as spacer to prevent the contact between two electrodes, which eliminated the employment of separator and greatly facilitated the mobility of ions.

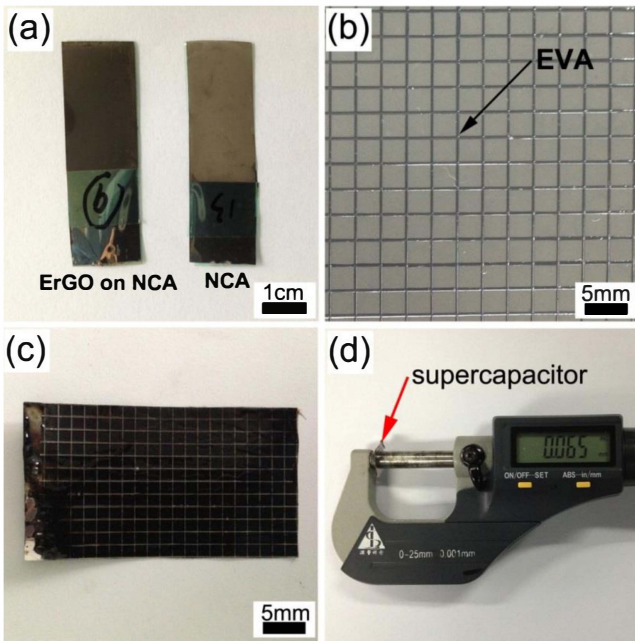


Fig. 3 (a) Photographic images of NCAs before and after electrochemical-deposition of ErGO. (b) NCAs substrate printed with EVA cofferdams. (c) Uniform ErGO layer deposited on NCA with EVA cofferdams. (d) Total thickness of the supercapacitor device with EVA cofferdams ( $65 \mu\text{m}$ ).

In order to assess the performance of GS, CV, GCD and EIS characterizations were conducted. A series of CV curves under different scan rate ranging from  $1 \text{ V/s}$  to  $100 \text{ V/s}$  are shown in Fig. 4a-b. The shape of CV curves exhibited nearly a symmetric rectangle at different scan rates, indicating excellent typical double layer capacitive characteristic. It is noteworthy that GS maintained almost perfectly symmetrically rectangular shape when the scan rate rose to  $100 \text{ V/s}$ , strongly suggesting the ultrahigh rate performance and the scan rate was much higher than most of the previously reported conditions [3, 12, 13]. It may be attributed to the

macroporous ErGO network shortening the diffusion pathway of ions. As shown in Fig. 4c, the GCD curves at different current densities exhibited nearly ideal triangle shape, and the IR drop calculated from the GCD curve under  $0.1 \text{ mA/cm}^2$  was only  $0.003 \text{ V}$ , suggesting a low equivalent series resistance, which may benefit from the good contact between ErGO and NCAs. In term of cycle stability, GS underwent 3000 cycles at  $1 \text{ V/s}$  scan rate, and the retention capacitance of GS was  $88\%$ , indicating excellent cycling stability. (Fig. 4d) To evaluate the ionic mobility in our symmetric supercapacitor, a supercapacitor assembled with a commercial separator was used as a control sample and the EIS results were compared. Different EIS curves of GS and supercapacitor with separator were given in Fig. 4e. (Inset: equivalent circuit model). According to the previous work, the curve in low frequency which showed a more vertical curve in Nyquist plot represents faster ion mobility [14]. The obvious difference was the section in low frequency, a supercapacitor with EVA cofferdams showed a more vertical line to Y axis compared to the supercapacitor with separator, suggesting better ion mobility. Energy and power density were two key parameters for supercapacitor, Fig. 4f showed the Ragone plot of symmetric supercapacitor with EVA cofferdams. The maximum energy density was up to  $0.04 \text{ mWh/cm}^3$ , which was more than one order of magnitude higher energy density compared with aluminum electrolytic capacitor. Meanwhile, the supercapacitor also exhibited excellent rate performance and ultrahigh power density (maximum value:  $1230 \text{ mW/cm}^3$ ), which was comparable to the aluminum electrolytic capacitor [15]. The above excellent electrochemical performance can be ascribed to three aspects: 1) macroporous ErGO network, providing fast transport for ions. 2) EVA cofferdams, eliminating the involvement of separator and promoting the mobility of ions. 3) aqueous electrolyte, guaranteeing superior ions' mobility compared with gel and solid electrolyte.

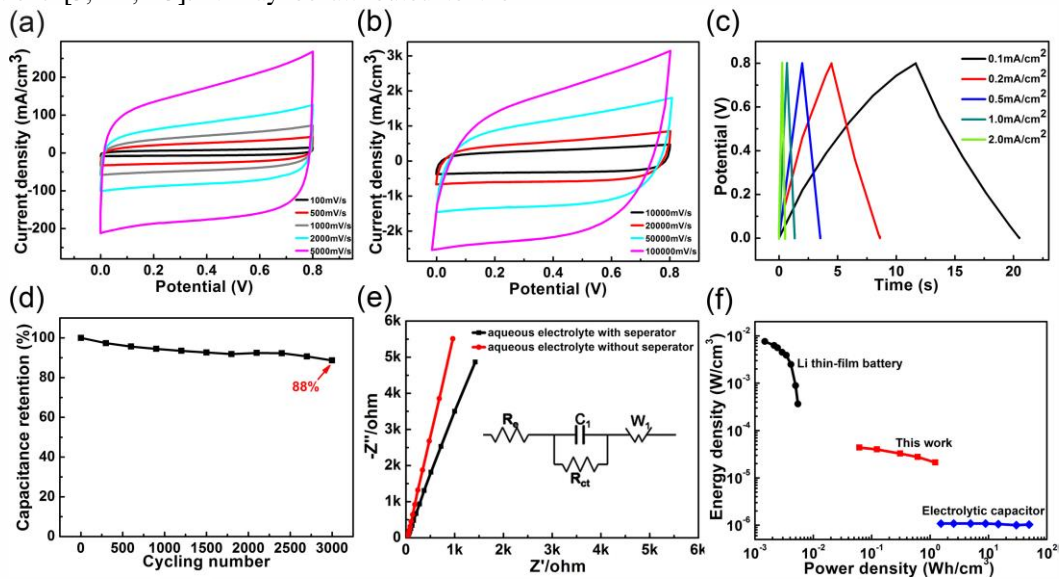


Fig. 4 (a), (b) CV curves of supercapacitor at different scan rate. (c) GCD curves of supercapacitor at different current densities. (d) Cycling stability of supercapacitor. (e) Nyquist plots of the EIS for supercapacitor. (Inset: equivalent circuit model). (f) Ragone plot of supercapacitor.

#### IV. CONCLUSION

In summary, we successfully fabricated ultrahigh power supercapacitor by combining NCAs deposited uniform macroporous ErGO network with stencil printing process. Due to the involvement of stencil printing process, the EVA cofferdams were constructed on NCAs substrates, aiming at eliminating the involvement of commercial separator, which not only prevented the contact between two electrodes but also promoted the mobility of ions. A series of electrochemical tests demonstrated that GS assembled with two identical ErGO electrodes showed excellent rate performance, superior ion migration and ultrahigh power density, strongly supporting the importance of morphology of graphene and smart design of supercapacitor. As the process is so simple, this technology can meet the demand of applications with high power and inspire the development of other energy storages to achieve better performance.

#### ACKNOWLEDGMENT

The authors thank National Nature Science Foundation of China Project No. 51202120, Shenzhen Government Technical Project No. JCYJ20130402145002411, Shenzhen Peacock Plan Project NO.KQCX20120814155245647, and Nanshan District "Rising Stars" Project No. KC2014JSQN0010A for financial supports.

#### REFERENCES

[1] P. Simon and Y. Gogotsi, "Materials for electrochemical capacitors," *Nat Mater.*, vol. 7, pp. 845-854, November 2008.

[2] A. K. Geim, "Graphene: status and prospects," *Science.*, vol. 324, pp. 1530-1534, June 2009.

[3] C. Liu, Z. Yu, D. Neff, A. Zhamu, and B. Z. Jang, "Graphene-based supercapacitor with an ultrahigh energy density," *Nano Lett.*, vol. 10, pp. 4863-4868, November 2010.

[4] Y. Meng, Y. Zhao, C. Hu, H. Cheng, Y. Hu, Z. Zhang, et al., "All-graphene core-sheath microfibers for all-solid-state, stretchable fibriform supercapacitors and wearable electronic textiles," *Adv. Mater.*, vol. 25, pp. 2326-2331, March 2013.

[5] K. Sheng, Y. Sun, C. Li, W. Yuan, and G. Shi, "Ultrahigh-rate supercapacitors based on electrochemically

reduced graphene oxide for ac line-filtering," *Sci Rep.*, vol. 2, 247-251, December 2012.

[6] J. Chen, K. Sheng, P. Luo, C. Li, and G. Shi, "Graphene hydrogels deposited in nickel foams for high-rate electrochemical capacitors," *Adv. Mater.*, vol. 24, pp. 4569-4573, July 2012.

[7] Y. Wang, Z. Shi, Y. Huang, Y. Ma, C. Wang, M. Chen, et al., "Supercapacitor devices based on graphene materials," *J Phys Chem C*, vol. 113, pp. 13103-13107, July 2009.

[8] J. J. Yoo, K. Balakrishnan, J. Huang, V. Meunier, B. G. Sumpter, A. Srivastava, et al., "Ultrathin planar graphene supercapacitors," *Nano letters*, vol. 11, pp. 1423-1427, March 2011.

[9] W. Lv, D.-M. Tang, Y.-B. He, C.-H. You, Z.-Q. Shi, X.-C. Chen, et al., "Low-temperature exfoliated graphenes: vacuum-promoted exfoliation and electrochemical energy storage," *ACS Nano.*, vol. 3, pp. 3730-3736, October 2009.

[10] Z. Su, C. Yang, B. Xie, Z. Lin, Z. Zhang, J. Liu, et al., "Scalable fabrication of MnO<sub>2</sub> nanostructure deposited on free-standing Ni nanocone arrays for ultrathin, flexible, high-performance microsupercapacitor," *Energy Environ. Sci.*, vol. 7, pp. 2652-2659, May 2014.

[11] Y. Shao, J. Wang, M. Engelhard, C. Wang, and Y. Lin, "Facile and controllable electrochemical reduction of graphene oxide and its applications," *J. Mater. Chem.*, vol. 20, pp. 743-748, November 2010.

[12] L.-F. Chen, Z.-H. Huang, H.-W. Liang, W.-T. Yao, Z.-Y. Yu, and S.-H. Yu, "Flexible all-solid-state high-power supercapacitor fabricated with nitrogen-doped carbon nanofiber electrode material derived from bacterial cellulose," *Energy Environ. Sci.*, vol. 6, pp. 3331-3338, August 2013.

[13] Z. Niu, L. Zhang, L. Liu, B. Zhu, H. Dong, and X. Chen, "All-solid-state flexible ultrathin micro-supercapacitors based on graphene," *Adv. Mater.*, vol. 25, pp. 4035-4042, May 2013.

[14] L. Qu, Y. Zhao, A. M. Khan, C. Han, K. M. Hercule, M. Yan, et al., "Interwoven three-dimensional architecture of cobalt oxide nanobrush-graphene@Ni<sub>x</sub>Co<sub>2x</sub>(OH)<sub>6x</sub> for high-performance supercapacitors," *Nano Lett.*, February 2015.

[15] M. F. El-Kady and R. B. Kaner, "Scalable fabrication of high-power graphene micro-supercapacitors for flexible and on-chip energy storage," *Nat. Commun.*, vol. 4, pp. 2037-2044, February 2013.